ISSN: 2357-0547 (Print)
ISSN: 2357-0539 (Online)

Research Article / JAPR / Sec. D
El-Habaak et al., 2025, 9 (4), 229-243

Journal of Advanced Pharmacy Research

Section D: Clinical Pharmacy & Pharmacology

Rebamipide Mitigates Paracetamol-Induced Hepatotoxicity by Modulating TLR4/NF-κB and STAT3 Signaling Pathways in Rats

Rana G. El-Habaak[1]*, Moahmed M. Elbadr[2], El-Sayed K. Elsayed[3]., Nashwa Hamad [4], Engy M. El Morsy[3]

[1] *The Therapeutic Medicine Administration, Health Directorate, Assiut, Ministry of Health and Population, 71515, Egypt*
[2] *Department of Medical Pharmacology, Faculty of Medicine, Assiut University, Assiut, 71515, Egypt*
[3] *Department of Pharmacology and Toxicology, Faculty of Pharmacy, Helwan University, Ein Helwan, Cairo, 11795, Egypt*
[4] *Department of Pathology, Faculty of Veterinary Medicine, Assiut University, Assiut, 71515, Egypt.*

***Corresponding author:** El-Habaak G. Rana, The Therapeutic Medicine Administration, Health Directorate, Assiut, Ministry of Health and Population, 71515, Egypt. Tel.: +0201027217071*
E-mail address: rana.hamed@pharm.helwan.edu.eg

Submitted on: 29-06-2025; Revised on: 19-07-2025; Accepted on: 31-07-2025

To cite this article: El-Habaak, R. G, Elbadr, M. M.; El-Sayed, K. E.; Nashwa, H.; El Morsy E.M. Rebamipide Mitigates Paracetamol-Induced Hepatotoxicity by Modulating TLR4/NF-κB and STAT3 Signaling Pathways in Rats. *J. Adv. Pharm. Res.* **2025**, *9* (4), 229-243. DOI: 10.21608/aprh.2025.398843.1323

ABSTRACT

Background: Rebamipide (Reba) is an amino acid analog approved for gastric mucosal protection. It exhibits anti-inflammatory and antioxidant properties by inhibiting neutrophil adhesion, diminishing the secretion of inflammatory cytokines, and limiting the production of reactive oxygen species (ROS). **Objective:** The present study aimed to evaluate the hepatoprotective effects of Reba in the context of paracetamol (PCM)-induced acute liver failure in rats. **Methods:** Animals were categorized into five distinct groups: control (vehicle), PCM (2 g/kg, p.o. on day 14), NAC (200 mg/kg for 13 days plus PCM on day 14), and Reba-treated groups (100 mg/kg and 200 mg/kg for 13 days plus PCM on day 14). **Results:** Reba treatment at both doses resulted in an enhancement of liver function. This is indicated by reduced serum transaminase levels, liver weight (LW), and the liver weight-to-body weight ratio (LW/BW). Oxidative stress was mitigated, evidenced by decreased malondialdehyde (MDA) and elevated glutathione (GSH) and catalase (Cat) levels. Reba also exerted a strong anti-inflammatory effect, significantly lowering TNF-α, IL-6, and NF-κB levels. Additionally, Reba decreased hepatic apoptosis, marked by downregulation of pro-apoptotic Bax and Caspase3 along with the upregulation of anti-apoptotic Bcl2. The compound also suppressed the TLR4-MyD88-NF-κB signaling pathway and significantly attenuated activation of the STAT3/p-STAT3 axis. **Conclusion:** Reba effectively protects against PCM-induced hepatic injury due to its anti-inflammatory, antioxidant, and anti-apoptotic actions. These findings indicate its promise as a therapeutic option for preventing acute hepatic damage.

Keywords: *Rebamipide; Paracetamol; Hepatoprotection; Oxidative stress; Inflammation; Apoptosis; TLR4-MyD88-NF-κB; STAT3.*

INTRODUCTION

The liver is regarded as one of the vital organs in the human body due to its substantial function in drug elimination and metabolism[1]. The liver is a key location for drug metabolism, where it detoxifies endogenous compounds and byproducts of metabolic processes via phases I and II reactions. The metabolism of drugs and xenobiotics to nontoxic substances in the liver is essential for the body's proper function. Changes in these

statuses lead to a shift in metabolism toward the production of oxidants, which bind to lipids or nuclear proteins, resulting in mutations, membrane damage, and modifications in enzyme activity, ultimately culminating in organ dysfunction. One of the most common reasons for human hepatic injury is pharmaceutical medications and herbal supplements, which significantly contribute to the generation of oxidants [2].

One potentially fatal condition is acute liver disease, which is characterized by abrupt liver dysfunction in individuals without any prior history of liver disease [3]. Many factors, including chemical exposure, adverse drug reactions, and viral infections, can lead to acute liver damage. Various categories of pharmaceuticals have the potential to induce liver damage, such as nonsteroidal anti-inflammatory drugs (NSAIDs), anti-infective agents, cancer treatment medications, hormonal therapies, immunosuppressive drugs, as well as certain herbal supplements [4–6].

Paracetamol (PCM) serves as a frequently employed analgesic and antipyretic, being relatively safer than NSAIDs; however, excessive intake can result in various liver injuries, ranging from minor liver enzyme elevations to severe liver failure and encephalopathy [7]. About 95% of PCM undergoes metabolism in the liver through glucuronidation and sulfation. Approximately 5% of PCM is converted into N-acetyl-p-benzoquinone imine (NAPQI), a toxic metabolite, via an oxidation reaction that further binds to cysteine, DNA, and lipids [8,9]. NAPQI is detoxified by glutathione (GSH) to form a mercapturic metabolite excreted by the kidney. In the case of PCM toxicity, the intracellular GSH is depleted, resulting in a relative shunting of PCM metabolism toward oxidation [10], which leads to an increase in the NAPQI amounts. Higher levels of NAPQI bind to hepatic sulfhydryl-containing proteins and enzymes, exerting oxidative damage and producing hepatocyte destruction, which can rapidly progress to acute liver failure [11,12]. N-acetyl cysteine (NAC) is the specific antidote against PCM overdose; however, it should be administered as early as possible to prevent disease progression [13].

Numerous research studies suggest that inflammation, oxidative stress, and apoptosis are involved in the hepatic injury resulting from PCM [14–16]. Furthermore, the activation of Toll-like receptors/nuclear factor-κB (TLR/NF-κB) leads to both pro-inflammatory gene transcription and anti-apoptotic proteins, increasing [17]. The activation of TLR-4 triggers the myeloid differentiation primary response protein (MyD88), which promotes the translocation of NF-κB into the nucleus and up-regulation of the expression of many pro-inflammatory cytokines, such as interleukin-6 (IL-6) and tumor necrosis factor-alpha (TNF-α) [18,19]. The activated NF-κB and produced IL-6 will activate STAT3[20–22] through the receptor-associated JAKs, leading to activation, dimerization, and translocation of STAT into the nucleus [20] together with a subsequent increase in the transcription of inflammatory cytokines, apoptosis, and cellular signaling [23].

Rebamipide (Reba) is an amino acid analog of 2(1H)-quinolinone [24] which is used as a gastroprotective drug to treat gastritis, peptic ulcer, and mucosal injury. It enhances gastric defense mechanisms by increasing gastric mucus production [25,26] and prostaglandin synthesis [27,28]. Moreover, it decreases the expression of neutrophil adhesion molecules and inhibits the secretion of TNF-α, demonstrating anti-inflammatory activity. [29,30]. The ability of Reba to scavenge free radicals and suppress reactive oxygen species explains its antioxidant activity [22,31,32] . Several previous studies have demonstrated its protective effect against nephrotoxicity [33], small bowel injury [27,34], peripheral arthritis [35], asthma [36], and bladder inflammation [37] by suppressing oxidative stress and inflammatory reaction in a dose-dependent manner. Furthermore, Reba promotes the healing of colonic ulceration through enhanced epithelial restitution and elevates the number of mucin-like substances in the conjunctiva. Accordingly, the current study aims to investigate the potential protective impact of Reba against PCM-induced liver damage. Moreover, the aim extends to inspecting the involved molecular pathways.

MATERIAL AND METHODS

Drugs

PCM was acquired from GlaxoSmithKline (GSK, Brentford, UK), Reba was sourced from Otsuka Pharmaceutical Co., Ltd. (Japan), and NAC was procured from AK Scientific Inc. (USA).

Animals

Adult male albino Wistar rats, weighing between 180 and 200 g, were used in this study and obtained from the Egyptian Organization of Biological Products and Vaccines Unit (Helwan, Egypt). Animals were housed for 2 weeks in the laboratory room before testing. The animals were kept in a regular environment: temperature (23 ± 4°C), humidity (60% ± 10%), and alternating 12-hour light and dark cycles. Animals were fed a standard pellet diet, and tap water was allowed ad *libitum*. The Faculty of Pharmacy, Helwan University's animal care and use committee approved the animal care and experimental protocols (Approval #02A2023). The study was done following the guide for the care and use of laboratory animals published by the US National Institutes of Health (NIH publication No. 85-23, revised 2011).

Experimental Design

The rats were allocated into five groups (n = 6) as follows: Control group - The rats received the vehicle (1% Tween 80 solution) orally by gavage for 14 days.

PCM group: The rats received the vehicle orally by gavage for 13 days and PCM (2 g/kg p.o.) on the 14th day. NAC group: The rats received NAC (200 mg/kg/p.o.) for 13 days and were given PCM (2 g/kg/p.o.) on the 14th. Reba 100 mg group: The rats received Reba (100 mg/kg/p.o.) for 13 days and were given PCM 2 g/kg on the 14th day. Reba 200 mg group: The rats received Reba (200 mg/kg/p.o.) for 13 days and were given PCM (2 g/kg/p.o.) on the 14th. The selection of the doses was according to the previous studies for PCM [38], NAC [39], and Reba [40].

Blood samples and tissue collection

Blood samples were collected from the tail vein of the rat 24 hours after the last dose of the drug or vehicle was administered, and they were allowed to clot. After centrifuging the blood for 10 minutes at 3000 rpm, the serum was separated and stored at -80°C until it was needed for further analysis. The animals underwent weighing before euthanasia via cervical dislocation. The liver was promptly removed and rinsed in an ice-cold saline solution before weighing. A portion of the liver was preserved in 10% neutral buffered formalin for immunohistochemistry and histopathological investigations. A Teflon homogenizer (Glas-Col®, USA) was used to blend another piece of the liver tissue in a cold phosphate buffer (0.1 M, pH 7.4) to create a 10% mixture. This blend was spun in a centrifuge for 10 minutes at 3000 rpm at 4°C to estimate biochemical parameters.

Estimation of liver index

The ratio of liver weight to body weight was calculated and expressed as g/g. Subsequently, the liver index was determined using the formula

Liver index = (liver weight/body weight) × 100

Assessment of liver function tests

The concentrations of aspartate aminotransferase (AST), alanine aminotransferase (ALT), alkaline phosphatase (ALP), and total bilirubin (TB) serum were measured using colorimetric methods with commercial-specific kits, Cat. #260 001, Cat. #264001, Cat. #AP 10 20, and Cat. #BR1111, respectively, supplied from Spectrum Diagnostics, Egypt.

Evaluation of oxidative stress markers

The levels of malondialdehyde (MDA), catalase (CAT), and glutathione (GSH) were measured using a commercial kit identified as Cat. #MD 25 29 and Cat. #CA 25 17 supplied from Spectrum Diagnostics, Egypt, and CAS #2110027, supplied from Sigma Aldrich, respectively.

Estimation of inflammatory markers

Tumor necrosis factor (TNF-α) and Interleukin 6 (IL-6) levels were determined utilizing ELISA kits (Cat. #MBS269892, MYBIOSOURCE, USA) and (Cat. #CSB-E11987r, CUSABIO, China), respectively.

Gene expression and quantitative RT-PCR for TLR4

Total RNA was extracted from cell cultures at different time intervals using the RNAiso Plus reagent (Takara Bio, Inc., Japan). To eliminate the genomic DNA, RNA was treated with RNase-free DNase before it was eluted from the column. RNA quantification and quality assessment are performed at 260 and 280 nm. All RNA samples are distinguished by their high-quality attributes. They were subsequently reverse-transcribed into cDNA using a kit (GoTaq® 1-Step RT-qPCR System). The Perfect Real Time technique was implemented following the manufacturer's instructions. The target gene primer sequence was as follows. TLR4 PRIMER: NM_019178.1 F: 5′- TCA TGC TTT CTC ACG GCC TC -3′ R: 5′- AGG AAG TAC CTC TAT GCA GGG AT-3′ GAPDH PRIMER: NM_017008.4 F: 5′-CAT CAC TGC CAC TCA GAA GAC TG-3′ R: 5′-ATG CCA GTG AGC TTC CCG TTC AG-3′.

Assessment of MYD88, STAT3, and Phospho-STAT3 by Western Blot Analysis

Proteins were isolated utilizing the Cell Lytic Nuclear Extraction Kit (Sigma-Aldrich, St. Louis, MO, USA). The quantification of these proteins was carried out with a microplate bicinchoninic acid protein assay kit (Thermo Fisher Scientific, Inc., Rockford, USA). All wash buffers and membranes were treated with 5% bovine serum albumin (BSA) in Tris-buffered saline with Tween 20 (TBST: 50 mM Tris, pH 7.6, 150 mM NaCl, and 0.1% Tween 20). Then, they were incubated overnight at 4°C in 5% BSA in TBST with a MYD88 monoclonal antibody Cat #67969-1-Ig, a STAT3 polyclonal antibody Cat #10253-2-AP, and a phospho-STAT3 monoclonal antibody Cat #Tyr705 (D3A7) XP for one hour. They were then washed three times with TBS and incubated with a peroxidase-conjugated goat anti-rabbit secondary antibody (1:5,000; 111-035-003; Jackson Immunoresearch, Baltimore, MD, USA) for two hours at room temperature. Immunolabeling was identified by using enhanced chemiluminescence reagents (Amersham Biosciences; GE Healthcare, Little Chalfont, UK).

Histopathological assessment

Specimens obtained from the livers of all experimental groups were fixed in a 10% buffered formalin solution for 48 h. Routine histological processing (dehydration, clearing, and paraffin embedding) of the fixed specimens was accomplished. Sections measuring 5µm in thickness were cut using a microtome and subsequently stained with hematoxylin and eosin (H&E) for light microscopic examination [41].

Immunohistochemical analysis

The apoptotic protein expression, including Caspase3, Bax, Bcl2, and NF-κB as an inflammatory marker, was determined immunohistochemically. The paraffin sections of 4 µm thickness were dewaxed and hydrated in graded ethanol solutions. Slides were incubated in 3% hydrogen peroxide solution for 10 min to hinder the endogenous peroxidase activity. The samples were rinsed in phosphate-buffered saline and subsequently incubated for 10 minutes with 5% bovine serum albumin to prevent non-specific binding. Afterward, slides were incubated overnight at 4°C with a primary polyclonal anti-rat antibody specific for Caspase3 (1:500, Thermo Fisher Scientific, USA), Bax (1:200, Bioss Antibodies, European company), Bcl2 (1:200, Biogenex Diagnostics, India), and NF-κB (1:200, Biogenex Diagnostics, India). Subsequently, the sections were incubated with biotinylated secondary antibodies and horseradish peroxidase-labeled streptavidin. Then, the slides were incubated with 3,3′-diaminobenzidine (DAB), a substrate chromogen. The sections were washed in distilled water and counterstained with hematoxylin. Stained slides were visualized under a light microscope to check for brown-colored immunopositive cells [42]. The immunostaining was scored semi-quantitatively by evaluating the percentage of positively stained cells on 10 high-power fields/slides in 6 slides, representing six rats from each group (n=6). The proportion of positively stained cells was specified as follows: 0 = 0%, 1 = 10%, 2 = 10–30%, and 3 = >30%. Mean and standard error (SE) values were obtained for each group and statistically evaluated.

Statistical analysis

The data were presented as mean values ± SEM based on 6 observations. Statistical analysis and graphical representations were executed by using GraphPad Prism software (version 8). Group comparisons were conducted using one-way ANOVA, followed by Tukey's test. The significance level was set at a p-value of <0.05.

RESULTS

Effect of Reba on the body weight, liver weight, and liver index

Administering PCM at a dosage of 2 gm/kg to the rats led to a notable weight reduction of 4% ($p < 0.05$), with a significant increase in liver weight by 1.4-fold, and an increase in liver index by 1.5-fold when compared to the control group. Pre-treatment by NAC and Reba 100 mg and 200 mg significantly ameliorated the body weight reduction by 2.5%, 2.5%, and 1.7 %, respectively; elevated the liver weight by 26%, 22.6%, and 28 %, respectively; and elevated the liver index by 28%, 25%, and 30 %, respectively, compared to the PCM group (see **Table 1**).

Effect of Reba on the Liver Function Tests

Treatment with PCM caused liver injury, as indicated by a significant elevation in AST serum levels by 54%, ALT by 73%, ALP by 9.5%, and total bilirubin by 75% comparable to the control group at $p < 0.05$. Pre-treatment with NAC led to a significant reduction ($p < 0.05$) in AST serum levels by 29%, ALT by 10%, and total bilirubin by 23% when compared to the PCM group. Furthermore, pre-treatment with Reba 100 mg led to a notable decrease ($p < 0.05$) in AST by 26%, ALT by 12%, and total bilirubin by 17% in comparison to the PCM group. Meanwhile, pre-treatment with Reba 200 mg resulted in a significant reduction ($p < 0.05$) in AST by 44 %, ALT by 11%, and total bilirubin by 23% compared to the PCM group. Pretreatment with Reba 100 mg and 200 mg caused a no significant reduction in ALP serum level in comparison with the PCM-treated group (see **Figs. 1a-d**).

Effect of Reba on Oxidative Stress Markers

Administration of PCM exerted oxidative damage with a significant ($p < 0.05$) elevation in MDA by 1.5-fold and a decline in GSH level by 14% and catalase activity by 17%, when comparable to the control group. In contrast, pre-treatment with NAC improved the oxidative hepatic injury of PCM in a dose-dependent manner, showing a significant ($p < 0.05$) reduction in MDA by 17% as well as an increase in GSH by 11% and catalase activity by 18% compared to the PCM-treated group. Additionally, pre-treatment with Reba at 100 mg resulted in a notable 21% reduction in MDA compared to the PCM group. Reba 200 mg ameliorated the oxidative injury with a significant ($p < 0.05$) decrease in the level of MDA by 16%, an alteration in GSH by 8%, and an increase in catalase by 14% compared to the PCM group **(**see **Figs. 2a-c).** Furthermore, treatment with Reba 200 mg resulted in a notable reduction in GSH levels (5%) and catalase activity (9%), compared to the Reba 100 mg-treated group.

Effect of tested drugs on inflammatory markers

The PCM-treated group exhibited a notable increase in TNF-α levels (1.7-fold) and IL-6 levels (1.5-fold), with a significant level of $p < 0.05$ compared to the control group. In contrast, the NAC-treated group exhibited a notable reduction in TNF-α levels by 38% and IL-6 levels by 29%, both with $p < 0.05$, relative to the PCM-treated group. Upon treatment with Reba at doses of 100 mg and 200 mg, the TNF-α level was significantly decreased ($p < 0.05$) by 16% and 22%, respectively and the level of IL-6 was significantly ($p < 0.05$) decreased by 10% and 19%, respectively, in comparison to the PCM-treated group **(**see **Figs. 3a, b)**. There was a significant decrease in TNF-α by 7% and IL-6 levels by 10 % in the Reba 200 mg group compared to the Reba 100 mg group.

Table 1. Effects of Reba on the body weight, liver weight, and liver index in PCM-induced hepatotoxicity in rats

Groups	Body weight (g)	Liver weight (g)	Liver index (%)
Control	218.66 ± 0.494	5.43 ± 0.066	2.46 ± 0.026
PCM (2 gm/kg)	210.33 ± 0.422[a]	7.53 ± 0.066[a,c]	3.57 ± 0.027[a,c]
NAC (200 mg/kg)	215.66±0.557[a,b]	5.56 ± 0.049[b]	2.55 ± 0.033[b]
Reba (100 mg/kg)	215.50 ± 0.342[a,b]	5.80 ± 0.036[a,b,c]	2.67 ± 0.016[a,b]
Reba (200 mg/kg)	213.83 ± 0.654[a,b]	5.45 ± 0.050 [b]	2.50 ± 0.025[b]

Data represented as mean ± SE of six observations; [a] significant difference from the control group; [b] significant difference from the PCM group; [c] significant difference from the NAC group.

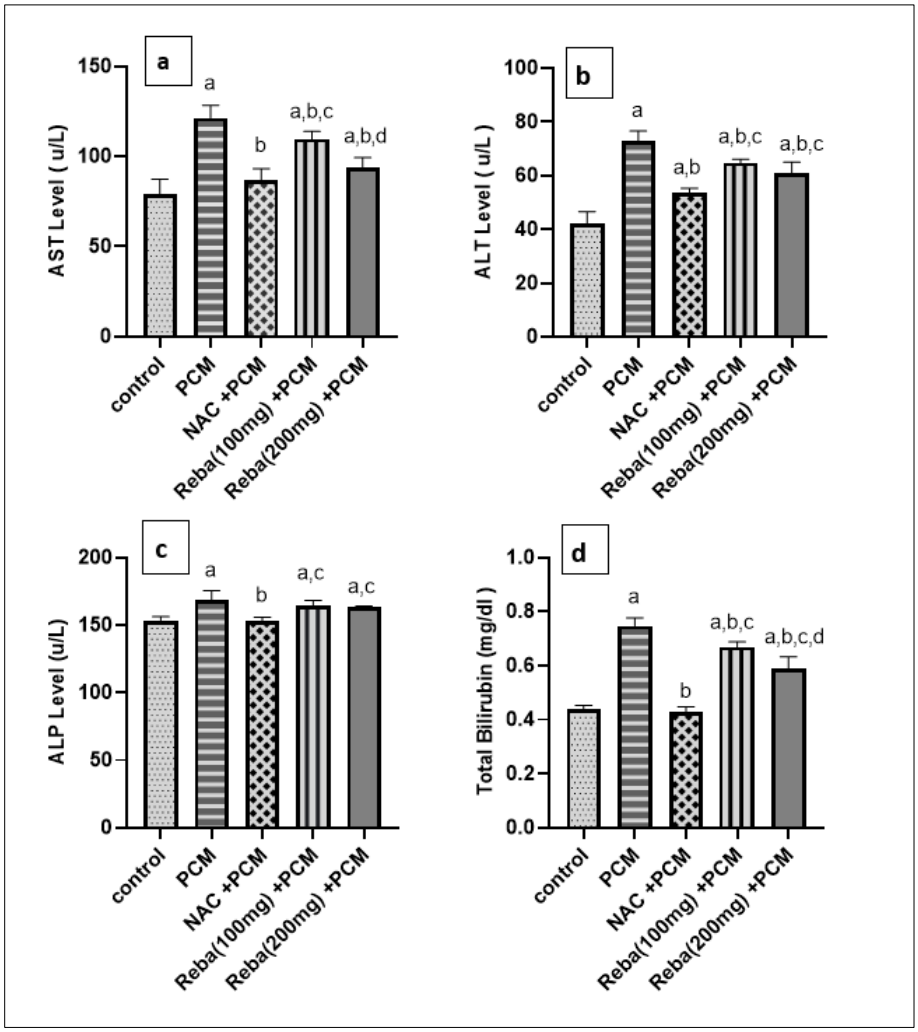

Figure 1. shows the effects of Reba and NAC on (a) aspartate aminotransferase (AST), (b) alanine aminotransferase (ALT), (c) alkaline phosphatase (ALP), and (d) total bilirubin (TB) in PCM-induced hepatotoxicity in rats. Data are represented as mean ± SE of six observations; a significant difference at $p < 0.05$ compared to the control group; b significant difference at $p < 0.05$ compared to the paracetamol group; c significant difference at $p < 0.05$ compared to the standard group; and d significant difference at $p < 0.05$ compared to the Reba 100 mg group.

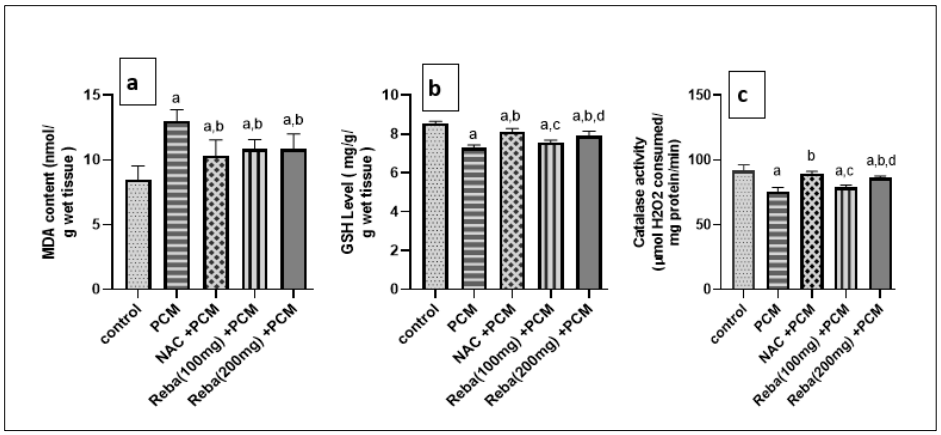

Figure 2. demonstrates the effects of Reba and NAC on the oxidative stress markers (a) malondialdehyde (MDA), (b) glutathione (GSH), and (c) catalase (CAT) in PCM-induced hepatotoxicity in rats. Data are represented as mean ± SE of six observations; a significant difference at $p < 0.05$ compared to the control group; b significant difference at $p < 0.05$ compared to the paracetamol group; c significant difference at $p < 0.05$ compared to the standard group; and d significant difference at $p < 0.05$ compared to the Reba 100 mg group.

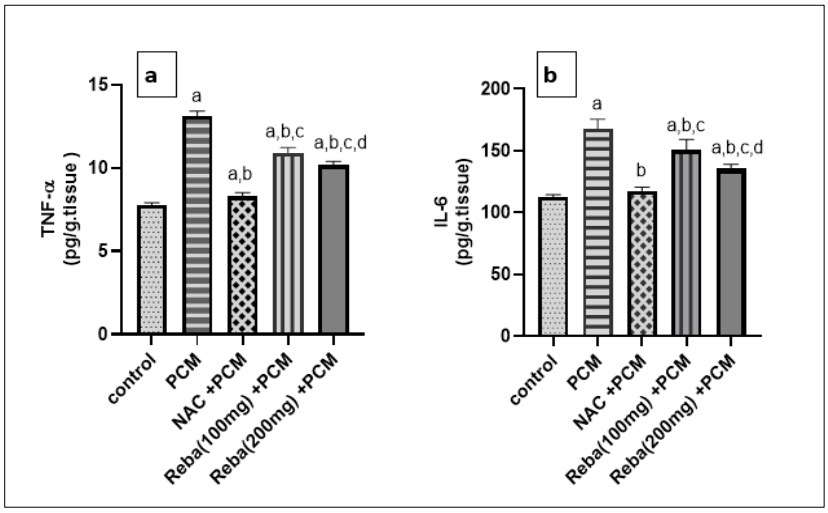

Figure 3. shows the effects of Reba and NAC on the inflammatory markers (a) tumor necrosis factor alpha (TNF-α) and (b) interleukin 6 (IL−6) in PCM-induced hepatotoxicity in rats. Data are represented as mean ± SE of six observations; a significant difference at $p < 0.05$ compared to the control group; b significant difference at $p < 0.05$ compared to the paracetamol group; c significant difference at $p < 0.05$ compared to the standard group; and d significant difference at $p < 0.05$ compared to the Reba 100 mg group.

Effect of the Tested Drugs on Hepatic TLR4 Expression (PCR) and STAT3, p-STAT3 and MYD88 Expressions

The administration of PCM led to a notable threefold increase in hepatic TLR4 expression ($p < 0.05$) compared to the control group. In contrast, the administration of NAC and Reba (100 mg, 200 mg) significantly decreased ($p < 0.05$) their level by 2.5-fold, 3.5-fold, and 3-fold, respectively, in comparison to PCM **(see Fig. 4).** Conversely, to assess the activation of the TLR4 pathway and to explore the mechanistic pathway underlying the hepatoprotective effect of Reba, Western blot analysis was utilized. As demonstrated in figures **(5a-d)**, the PCM-treated group exhibited a significant ($p < 0.05$) increase in STAT3 by 1.3-fold, p-STAT3 by 2.5-fold, and MYD88 expression by 2.8-fold, compared to the control group. In the meantime, a significant reduction ($p < 0.05$) in STAT3 levels was observed following pre-treatment with NAC, with STAT3 levels decreasing by 16%, p-STAT3 by 10%, and MYD88

expression by 19% in comparison to the PCM group. Following treatment with Reba at doses of 100 mg and 200 mg, a significant reduction ($p < 0.05$) is noted in STAT3 by 10% and 19%, p-STAT3 by 25% and 36%, and MYD88 expression by 30% and 36% relative to the PCM group. Notably, pre-treatment with Reba 200 mg led to a notable decline ($p < 0.05$) in p-STAT3 levels by 15% and a decrease in MYD88 expression by 8.7%, compared to the Reba 100 mg group.

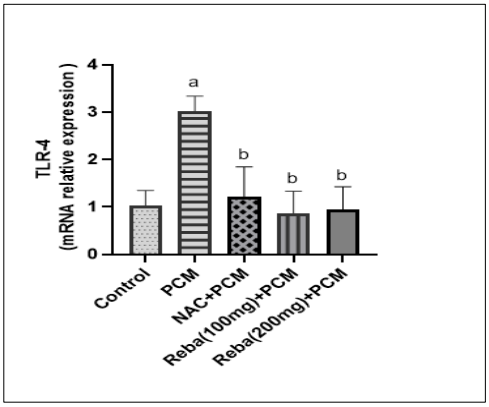

Figure 4. Illustrates the effects of Reba and NAC on the expression of hepatic Toll-like receptor 4 (TLR4) using PCR in PCM-induced hepatotoxicity. Data are represented as mean ± SE of six observations; a significant difference at $p < 0.05$ compared to the control group; b significant difference at $p < 0.05$ compared to the paracetamol group.

Histopathological observations

The microscopic study of the H&E-stained hepatic sections from control rats showed normally appearing central veins, blood sinusoids, and plates of hepatocytes with homogenous eosinophilic cytoplasm and centrally located basophilic nuclei. Portal areas, consisting of the bile ductules, portal vein, and hepatic artery, were also observed **(**see **Fig. 6a)**. In contrast, the PCM-received group exhibited marked histopathological alterations, including angiopathic changes characterized by abrasive congestion of central veins, blood sinusoids, and portal blood vessels **(**see **Figs. 6b, c)**. Moreover, extensive hemorrhages throughout the hepatic lobules were evident **(**see **Fig. 6d)**. Fatty degeneration and diffuse vacuolar degeneration of hepatocytes were detected **(**see **Fig. 6e)**. In addition, there were multifocal areas of hepatocyte coagulative necrosis in all examined sections of this group **(**see **Fig. 6f)**. There was evidence of remarkable infiltration of mononuclear cells throughout the hepatic parenchyma **(**see **Fig. 6g)** and perivascular **(**see **Fig. 6h)**. The portal areas displayed dilated bile ductules accompanied by periductular mononuclear cell infiltrates **(**see **Fig. 6i)**. Rats treated with the standard drug (NAC) revealed a normal histological structure of the hepatic lobules with mild sinusoidal congestion **(**see **Fig. 6j)**. Rats administered with Reba (100 mg) exhibited slight vascular congestion, diffuse vacuolar degeneration of hepatocytes of most examined lobules, and focal areas of mononuclear cell infiltration **(**see **Figs. 6k, l)**. Conversely, treatment with Reba 200 mg preserved the hepatic histomorphological appearance with mild sinusoidal dilatation in some lobules **(**see **Fig. 6m)**.

Immunohistochemical analysis of Bax, Bcl2, Caspase3, and NF-kB expression

Immunohistochemical analysis was accomplished in hepatic tissue sections to assess the apoptotic (Caspase3 and Bax), anti-apoptotic (Bcl2), and inflammatory (NF-kB) markers **(**see **Figs. 7-10)**. The PCM-treated tissue samples revealed a significant ($p < 0.05$) increase in the number of positively stained cells for Caspase3 by 5-fold, Bax by 5.6-fold, and NF-kB by 13-fold, and a significant ($p < 0.05$) decrease in the number of positively stained cells for Bcl2 by 66%, comparable to the control group. Treatment with NAC significantly ($p < 0.05$) decreased the expression of Caspase3 by 3-fold, Bax by 3-fold, and NF-kB by 6-fold, while it increased Bcl2 by 2.6-fold compared to the PCM-received group.

Rats treated with Reba 100 mg displayed moderately intense immunostaining of all examined markers with a significant Bcl2 increase by 1.8-fold, a significant decrease in Bax by 2-fold, and a non-significant decrease in Caspase3 and NF-kB comparable to the PCM-treated group. On the other hand, treatment with Reba 200 mg exhibited an immunoreaction comparable to the NAC-treated group, with a significant decline ($p < 0.05$) in the expression of Caspase3 by 2.5-fold, Bax by 2.4-fold, and NF-kB by 60% and an increase in Bcl2 by 2.5-fold compared to the PCM-received group.

DISCUSSION

PCM is widely used for its analgesic and antipyretic properties [43]. However, scientific evidence indicates that excessive consumption of PCM can lead to liver damage. In cases of overdose, toxicity often manifests initially as chest pain, vomiting, diarrhea, and, in some instances, shock, along with hepatic, myocardial, and renal failure [44,45]. Among the various drug-induced liver injuries, PCM overdose is the leading cause, accounting for over fifty percent of all acute liver failure cases [46]. This study assessed the hepatoprotective potential of Reba in relation to PCM-induced liver damage.

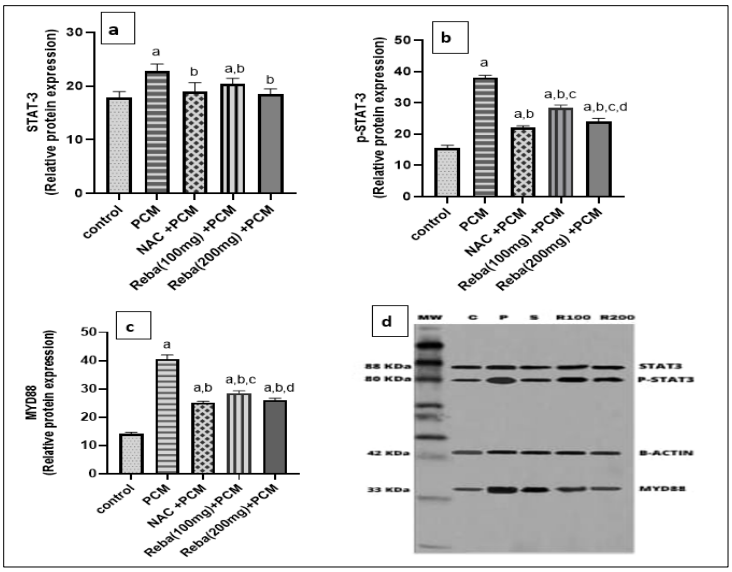

Figure 5. depicts the effects of NAC and Reba on (a) signal transducer and activator of transcription 3 (STAT3), (b) phosphorylated signal transducer and activator of transcription 3 (p-STAT3), (c) myeloid differentiation primary response 88 (MYD88) expressions in PCM-induced hepatotoxicity in rats, and (d) Western blot autoradiography of hepatic rat cell using STAT-3, p-STAT-3 and MYD88. Data are represented as mean ± SE of six observations; a significant difference at $p < 0.05$ compared to the control group; b significant difference at $p < 0.05$ compared to the paracetamol group; c significant difference at $p < 0.05$ compared to the standard group; and d significant difference at $p < 0.05$ compared to the Reba 100 mg group.

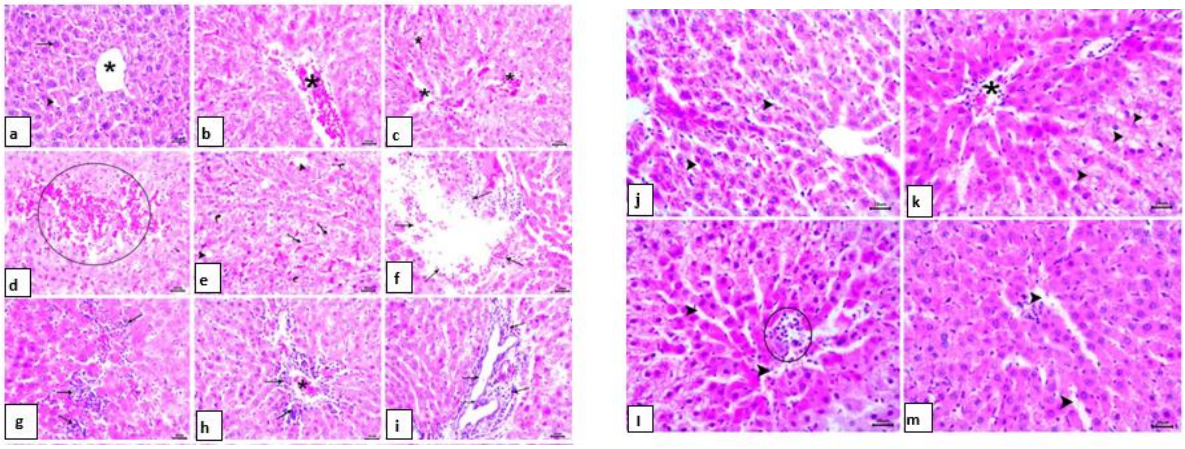

Figure 6. (a-i): Histopathological examination of the H&E-stained hepatic sections from control and PCM-treated rats. (a) Control liver demonstrating a normally appearing central vein (*) and hepatocytes with homogenous eosinophilic cytoplasm and centrally located basophilic nuclei (arrow) and blood sinusoids (arrowhead). (B-I) PCM-received group; (b) demonstrating congested central vein (*), (c) demonstrating dilated and congested blood sinusoids (*), (d) demonstrating extensive hemorrhages throughout the hepatic lobule (circle), (e) demonstrating fatty degeneration of hepatocytes (arrowhead), diffuse vacuolar degeneration (curved arrow), and focal area of coagulative necrosis (wavy arrow), (f) demonstrating hemorrhagic necrosed area (arrows), (g) demonstrating remarkable infiltration of mononuclear cells throughout the hepatic parenchyma (arrow), (h) demonstrating vascular congestion (*) along with perivascular mononuclear cells infiltration, and (i) demonstrating dilated bile ductule (wavy arrow) and periductular mononuclear cells infiltrates (arrow). (j-m): Histopathological examination of the H&E-stained hepatic sections from groups treated with the standard drug NAC, as well as Reba at doses of 100 mg and 200 mg. (j) Rats treated with standard medications demonstrated the normal histological structure of the hepatic lobules with only mild sinusoidal congestion (arrowhead). (k, l) rats treated with rebamipide (100 mg); (k) demonstrating congested central vein (*) and diffuse vacuolar degeneration of hepatocytes (arrowhead), while (l) demonstrating dilated sinusoids (arrowhead) along with a focal area of mononuclear cell infiltration (circle). (m) Treatment with rebamipide (200 mg) showed a well-preserved hepatic histomorphological appearance of the hepatic parenchyma, with only mild sinusoidal dilatation observed in certain lobules (arrowhead). Scale bar = 20 µm

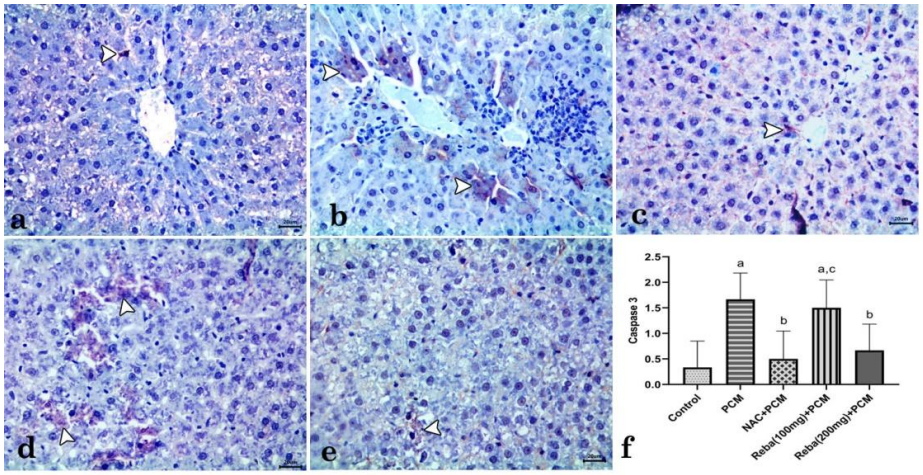

Figure 7. Immunohistochemical examination of hepatic tissue sections using anti-Caspase3 antibody. (a) The control group exhibited a mild and weak brown immunoreaction. (b) The PCM-received group demonstrated a pronounced immunoreaction. (c) Rats treated with standard drugs (NAC) demonstrated mild and weak immunoreaction. (d) Rats treated with Reba (100 mg) demonstrated moderately intense immunoexpression. (e) Rats treated with Reba (200 mg) demonstrated mild and weak immunoreaction. (f) Score of the percentage of immune-positive cells across all experimental groups. Data are represented as mean ± SE of six observations; a significant difference at $p < 0.05$ compared to the control group; b significant difference at $p < 0.05$ compared to the paracetamol group; c significant difference at $p < 0.05$ compared to the standard group; and d significant difference at $p < 0.05$ compared to the Reba 100 mg group.

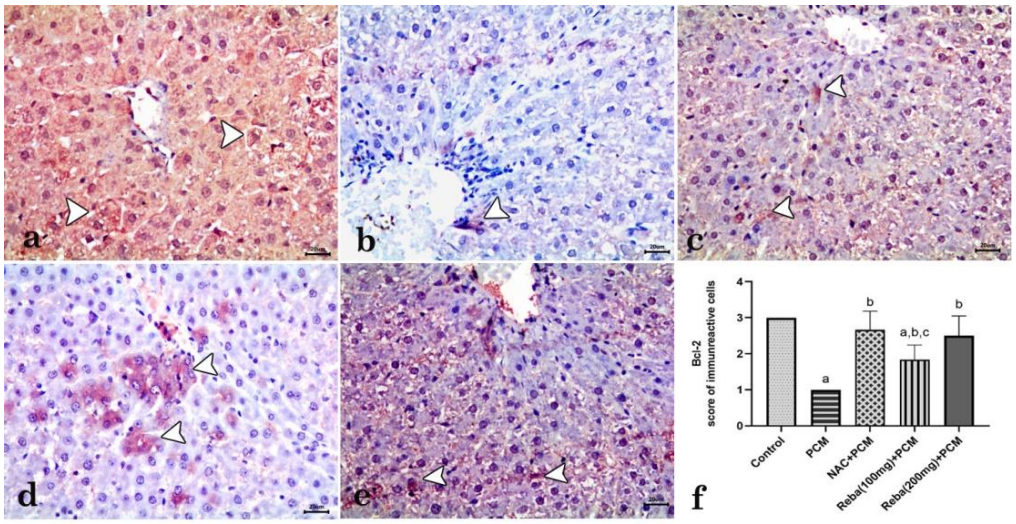

Figure 8. Immunohistochemical examination of hepatic tissue sections using anti-Bax antibody. (a) The control group demonstrated a mild and weak brown-colored immunoreaction. (b) The PCM-received group demonstrates a strong immunoreaction. (c) Rats treated with standard drugs (N-acetylcysteine) demonstrated mild and weak immunoreaction. (d) Rats treated with Reba (100 mg) demonstrated moderately intense immunoexpression. (e) Rats treated with rebamipide (200 mg) demonstrated mild and weak immunoreaction. (f) Score of the percentage of immune-positive cells in all experimental groups. Data are represented as mean ± SE of six observations; a significant difference at $p < 0.05$ compared to the control group; b significant difference at $p < 0.05$ compared to the paracetamol group; c significant difference at $p < 0.05$ compared to the standard group; and d significant difference at $p < 0.05$ compared to the Reba 100 mg group.

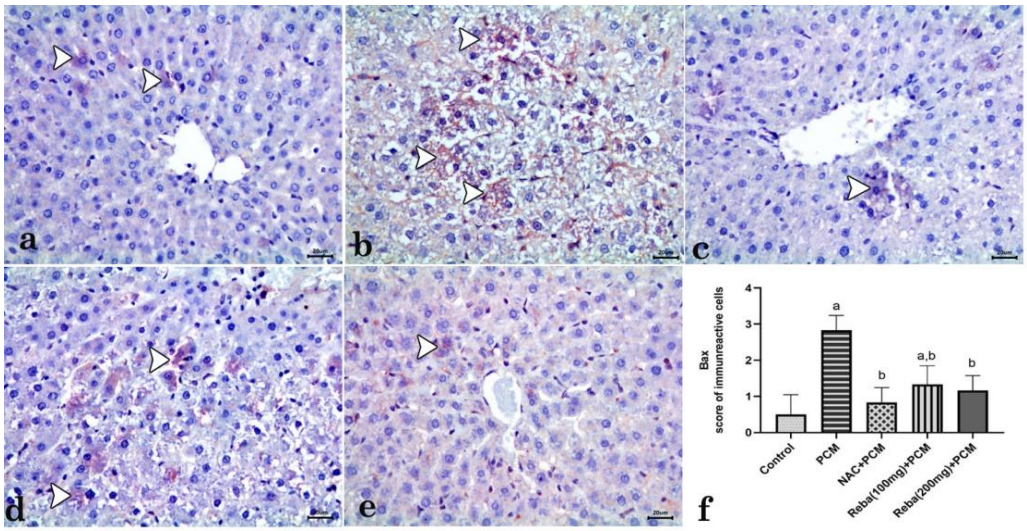

Figure 9. Immunohistochemical examination of hepatic tissue sections using anti-Bcl2 antibody. (a) The control group demonstrated a strong brown immunoreaction. (b) The PCM-received group demonstrated minimal immunoreaction. (c) Rats treated with the standard drug (NAC) demonstrated a strong immunoreaction. (d) Rats treated with Reba (100 mg) demonstrated moderately intense immunoexpression. (e) Rats treated with Reba (200 mg) demonstrated a strong immunoreaction. (f) Score of the percentage of immune-positive cells across all experimental groups. Data are represented as mean ± SE of six observations; a significant difference at $p < 0.05$ compared to the control group; b significant difference at $p < 0.05$ compared to the paracetamol group; c significant difference at $p < 0.05$ compared to the standard group; and d significant difference at $p < 0.05$ compared to the Reba 100 mg group.

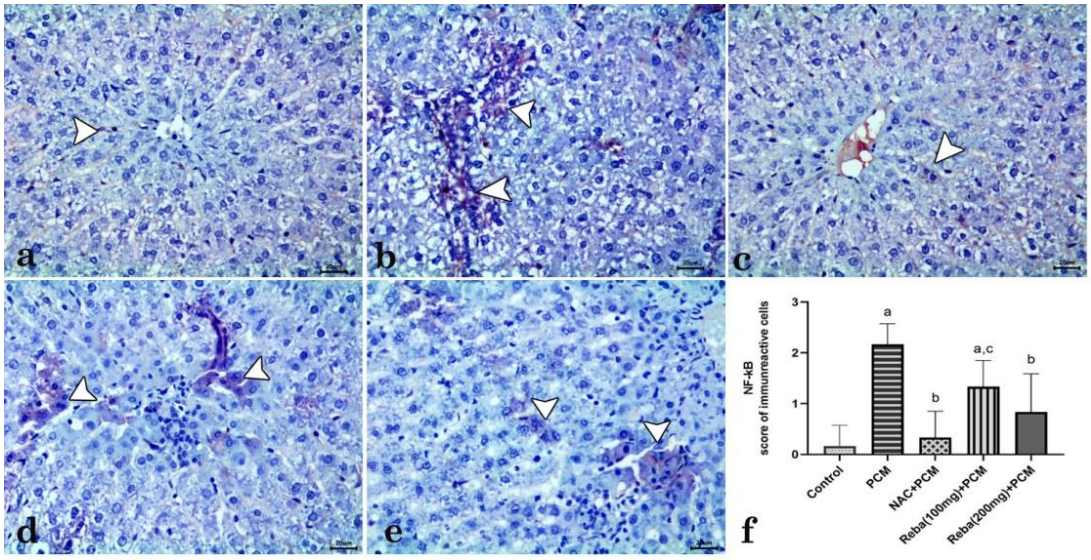

Figure 10. Immunohistochemical examination of hepatic tissue sections using anti-NF-kB antibody. (a) The control group demonstrated a mild and weak brown immunoreaction. (b) The PCM-received group demonstrated a strong immunoreaction. (c) Rats treated with standard drugs (NAC) demonstrated mild and weak immunoreaction. (d) Rats treated with Reba (100 mg) demonstrated moderately intense immunoexpression. (e) Rats treated with Reba (200 mg) demonstrated mild and weak immunoreaction. (f) Score of the percentage of immune-positive cells across all experimental groups. Data are represented as mean ± SE of six observations; a significant difference at $p < 0.05$ compared to the control group; b significant difference at $p < 0.05$ compared to the paracetamol group; c significant difference at $p < 0.05$ compared to the standard group; and d significant difference at $p < 0.05$ compared to the Reba 100 mg group.

The current research employed PCM to induce hepatotoxicity in rats, with the dosage established according to the reference dose [38]. Following administering PCM (2 g/kg) as a single oral dose, a noticeable increase in the LW/BW ratio was noticed, along with a marked elevation in serum biomarkers, including ALT, AST, ALP, and TB, which indicated significant hepatocellular damage. Damage-induced inflammation and extracellular matrix accumulation could be accountable for the effects shown on LW and the LW/BW ratio. The results were in harmony with the previous study of Mahmood et al. [47]. The rise in serum levels of liver enzymes and TB is attributed to the generation of reactive oxygen species by PCM overdose, which damages the hepatic cells through lipid peroxidation and alterations in cellular permeability [39]. The damaged hepatic cells were further documented by histopathological examinations, which revealed a marked decrease in viable hepatocytes, with extensive necrotic cells surrounding the centrilobular zone and reaching into the parenchymal region. These necrotic cells exhibited nuclear karyolysis and pyknosis, hallmarks of cell death.

The present investigation indicates that administering Reba at doses of 100 and 200 mg/kg demonstrated hepatoprotective effects, as evidenced by a significant reduction in liver function parameters (LW and LW/BW ratio). The hepatoprotective effects of Reba mainly stem from its strong antioxidant and anti-inflammatory attributes, which help prevent PCM-induced liver damage. By mitigating oxidative stress and inflammation, Reba preserves hepatocyte membrane integrity, limits transaminase release, and contributes to the normalization of histopathological changes.

The results indicated that PCM led to a significant increase in MDA levels while decreasing GSH and CAT activity compared with the control group. This reduction of cellular GSH is believed to be a result of the excessive formation of NAPQI due to PCM toxicity [48]. The elevated level of MDA is attributed to the higher degree of lipid peroxidation, which is associated with the oxidation of unsaturated fatty acids within the cell membrane [49,50]. Lipid peroxidation caused by the overproduction of reactive oxygen species (ROS) was evidenced by a decrease in GSH, an increase in hepatic MDA, and a reduction in catalase levels [51]. Our findings document the antioxidant effect of Reba, as evidenced by a significantly lower level of MDA alongside elevated levels of GSH and CAT. These results explain how Reba can inhibit lipid peroxidation and enhance the endogenous antioxidant system by mitigating the overproduction of ROS [52].

The present study further indicates that the administration of PCM resulted in an elevation of TNF-α and IL-6 within hepatic tissues, suggesting that inflammation is involved in the mediation of PCM-induced liver damage. TNF-α produced by the activated Kupffer cells has the potential to exacerbate inflammation and oxidative stress [53]. These findings are aligned with other results reported in the previous studies[54,55]. This inflammatory response is further supported by immunohistochemistry results, which demonstrated that PCM administration led to an increased expression of NF-κB, a key transcription factor involved in regulating pro-inflammatory cytokines, such as TNF-α and IL-6. The pretreatment with Reba demonstrated an anti-inflammatory effect, as evidenced by a notable reduction in the levels of TNF-α and IL-6. These results are consistent with other investigators who illustrated that Reba significantly reduced oxidative stress and decreased the elevation of TNF-α and IL-6 levels associated with liver injury [56]. Moreover, the capacity of Reba to inhibit NF-kB expression might be associated with its capability to modify the oxidative stress/NF-kB signaling pathway by rectifying redox imbalance [57,58].

Inflammation and oxidative stress are intricately interconnected processes contributing to apoptosis across various pathological conditions [59]. Oxidative stress and inflammatory mediators can upregulate pro-apoptotic proteins like Bax while simultaneously decreasing the levels of anti-apoptotic proteins such as Bcl2, thereby tilting the balance in favor of cell death [60]. Our study documented that PCM mediated apoptosis in hepatic tissues, as evidenced by a notable increase in Bax expression concurrently with a considerable decrease in Bcl2 expression. The results were in harmony with Ahmad et al. [61]. An increased Bax/Bcl2 ratio promotes apoptosis by inducing the permeabilization of the mitochondrial outer membrane, which results in the release of cytochrome c. This triggers apoptosome formation and the activation of Caspase9, which in turn activates Caspase3, and probably the key executioner of apoptosis. Thus, upregulated Bax and downregulated Bcl2 contribute to elevated Caspase3 levels, driving apoptotic cell death, as reported in our results. Pre-treatment with Reba caused a notable reduction in the levels of Bax and Caspase3 while causing upregulation of Bcl2. The results conformed to previous studies [62].

The TLR-MyD88 pathway is essentially involved in PCM-induced liver injury by recognizing damage-associated molecular patterns (DAMPs) that are released from necrotic hepatocytes. The MyD88-dependent signaling pathway triggers NF-κB activation, leading to the release of pro-inflammatory cytokines such as TNF-α and IL-6, which amplify liver inflammation and exacerbate tissue damage. This pathway contributes to hepatocyte apoptosis and necrosis, making it a potential target for mitigating PCM-induced hepatotoxicity [61]. TLR-4 receptors are extensively found in both hepatocytes and Kupffer cells. Research has shown that TLR-4 plays a significant role in the physiology and pathophysiology of the liver [63]. In

the current study, our results documented the involvement of the TLR-MyD88 pathway, evidenced by the overexpression of TLR4 and MyD88, which is in harmony with Du et al. [64]. Blocking the TLR-4 signaling pathway could be an effective approach for managing hepatic diseases. This study demonstrated that Reba suppressed TLR-4-mediated inflammatory responses [65] by blocking TNF-α and IL-6, obstructing the signaling pathway, and decreasing the expression of NF-κB [51].

The TLR-MyD88 signaling pathway is crucial for the regulation of the JAK-STAT signaling cascade. Upon activation by inflammatory cytokines, produced downstream of TLR-MyD88 signaling, the Janus kinase (JAK) phosphorylates signal transducer and activator of transcription 3 (STAT3), leading to its activation (p-STAT3). Once phosphorylated, STAT3 moves to the nucleus, where it influences gene expression related to cell survival, inflammation, and immune responses [64]. Persistent activation of the TLR-MyD88/STAT3 axis contributes to chronic inflammation, hepatocyte injury, and liver damage, such as PCM-induced liver toxicity. Therefore, targeting this pathway may help mitigate excessive inflammatory responses and tissue damage. Treatment with Reba significantly ameliorated the STAT3 axis, as demonstrated by the significantly reduced levels of STAT3 and p-STAT3. Therefore, the significant reduction in p-STAT3 and STAT3 levels following Reba treatment highlights its anti-inflammatory and hepatoprotective properties. By modulating the STAT3 axis, Reba likely prevents excessive cytokine-driven liver damage**,** making it a promising therapeutic agent against PCM-induced hepatotoxicity.

CONCLUSION

The present study emphasizes the hepatoprotective potential of Reba against PCM-induced liver injury through its antioxidant, anti-inflammatory, and anti-apoptotic properties**.** Pre-treatment with Reba demonstrated protective effects by significantly reducing liver enzyme levels, restoring antioxidant defenses such as GSH and catalase, and mitigating oxidative stress-mediated damage by decreasing the level of MDA. Moreover, Reba downregulated inflammatory mediators (TNF-α and IL-6), suppressed NF-κB expression, and modulated apoptosis by decreasing Bax and Caspase3 levels while increasing Bcl2 expression. The involvement of the TLR-MyD88 and JAK-STAT3 pathways in PCM-induced liver injury was also confirmed, with Reba effectively inhibiting TLR-4/MyD88/NF-κB activation and reducing STAT3 and p-STAT3 expression. These results indicate that Reba possesses hepatoprotective properties by modulating oxidative stress, inflammatory responses, and apoptotic pathways, thereby establishing it as a potential treatment option for PCM-induced hepatotoxicity.

Funding Acknowledgments

This research did not receive any specific grant from funding agencies in the public, commercial, or non-profit sectors.

Conflict of interest

The author declares that there isn't any conflict of interest regarding the publication of this paper.

REFERENCES

1. Pandit, A.; Sachdeva, T.; Bafna, P. Drug-Induced Hepatotoxicity: A Review. *J Appl Pharm Sci* **2012**, doi:10.7324/JAPS.2012.2541.
2. Upadhyay, G.; Gupta, S.P.; Prakash, O.; Singh, M.P. Pyrogallol-Mediated Toxicity and Natural Antioxidants: Triumphs and Pitfalls of Preclinical Findings and Their Translational Limitations. *Chem Biol Interact* **2010**, *183*, 333–340, doi:10.1016/j.cbi.2009.11.028.
3. Shahzad, M.F.; Xu, S.; Lim, W.M.; Yang, X.; Khan, Q.R. Artificial Intelligence and Social Media on Academic Performance and Mental Well-Being: Student Perceptions of Positive Impact in the Age of Smart Learning. *Heliyon* **2024**, *10*, doi:10.1016/j.heliyon.2024.e29523.
4. Yu, Y.; Mao, Y.; Chen, C.; Chen, J.; Chen, J.; Cong, W.; Ding, Y.; Duan, Z.; Fu, Q.; Guo, X.; et al. CSH Guidelines for the Diagnosis and Treatment of Drug-Induced Liver Injury. *Hepatol Int* **2017**, *11*, 221–241, doi:10.1007/s12072-017-9793-2.
5. ANDRADE, R.; LUCENA, M.; FERNANDEZ, M.; PELAEZ, G.; PACHKORIA, K.; GARCIARUIZ, E.; GARCIAMUNOZ, B.; GONZALEZGRANDE, R.; PIZARRO, A.; DURAN, J. Drug-Induced Liver Injury: An Analysis of 461 Incidences Submitted to the Spanish Registry Over a 10-Year Period. *Gastroenterology* **2005**, *129*, 512–521, doi:10.1016/j.gastro.2005.05.006.
6. Bunchorntavakul, C.; Reddy, K.R. Review Article: Herbal and Dietary Supplement Hepatotoxicity. *Aliment Pharmacol Ther* **2013**, *37*, 3–17, doi:10.1111/apt.12109.
7. Jacqz-Aigrain, E.; Anderson, B.J. Pain Control: Non-Steroidal Anti-Inflammatory Agents. *Semin Fetal Neonatal Med* **2006**, *11*, 251–259, doi:10.1016/j.siny.2006.02.009.
8. Jaeschke, H.; Bajt, M.L. Intracellular Signaling Mechanisms of Acetaminophen-Induced Liver Cell Death. *Toxicological Sciences* **2006**, *89*, 31–41, doi:10.1093/toxsci/kfi336.
9. Zhang, W.; Xu, M.; Feng, Y.; Mao, Z.; Yan, Z. The Effect of Procrastination on Physical Exercise among College Students—The Chain Effect of Exercise Commitment and Action Control. *International Journal of Mental Health Promotion*

2024, *26*, 611–622, doi:10.32604/ijmhp.2024.052730.
10. Bilzer, M.; Jaeschke, H.; Vollmar, A.M.; Paumgartner, G.; Gerbes, A.L. Prevention of Kupffer Cell-Induced Oxidant Injury in Rat Liver by Atrial Natriuretic Peptide. *American Journal of Physiology-Gastrointestinal and Liver Physiology* **1999**, *276*, G1137–G1144, doi:10.1152/ajpgi.1999.276.5.G1137.
11. Jaeschke, H.; Ramachandran, A. Reactive Oxygen Species in the Normal and Acutely Injured Liver. *J Hepatol* **2011**, *55*, 227–228, doi:10.1016/j.jhep.2011.01.006.
12. Athersuch, T.J.; Antoine, D.J.; Boobis, A.R.; Coen, M.; Daly, A.K.; Possamai, L.; Nicholson, J.K.; Wilson, I.D. Paracetamol Metabolism, Hepatotoxicity, Biomarkers and Therapeutic Interventions: A Perspective. *Toxicol Res (Camb)* **2018**, *7*, 347–357, doi:10.1039/c7tx00340d.
13. Janes, J.; Routledge, P.A. Recent Developments in the Management of Paracetamol (Acetaminophen) Poisoning. *Drug Saf* **1992**, *7*, 170–177, doi:10.2165/00002018-199207030-00002.
14. An, P.; Wei, L.-L.; Zhao, S.; Sverdlov, D.Y.; Vaid, K.A.; Miyamoto, M.; Kuramitsu, K.; Lai, M.; Popov, Y. V. Hepatocyte Mitochondria-Derived Danger Signals Directly Activate Hepatic Stellate Cells and Drive Progression of Liver Fibrosis. *Nat Commun* **2020**, *11*, 2362, doi:10.1038/s41467-020-16092-0.
15. Bhogal, R.H.; Curbishley, S.M.; Weston, C.J.; Adams, D.H.; Afford, S.C. Reactive Oxygen Species Mediate Human Hepatocyte Injury during Hypoxia/Reoxygenation. *Liver Transplantation* **2010**, *16*, 1303–1313, doi:10.1002/lt.22157.
16. Jaeschke, H.; Mitchell, J.R. Mitochondria and Xanthine Oxidase Both Generate Reactive Oxygen Species in Isolated Perfused Rat Liver after Hypoxic Injury. *Biochem Biophys Res Commun* **1989**, *160*, 140–147, doi:10.1016/0006-291X(89)91632-X.
17. Joosten, L.A.B.; Abdollahi-Roodsaz, S.; Dinarello, C.A.; O'Neill, L.; Netea, M.G. Toll-like Receptors and Chronic Inflammation in Rheumatic Diseases: New Developments. *Nat Rev Rheumatol* **2016**, *12*, 344–357, doi:10.1038/nrrheum.2016.61.
18. Ahmed-Hassan, H.; Abdul-Cader, M.S.; Sabry, M.A.; Hamza, E.; Abdul-Careem, M.F. Toll-like Receptor (TLR)4 Signalling Induces Myeloid Differentiation Primary Response Gene (MYD) 88 Independent Pathway in Avian Species Leading to Type I Interferon Production and Antiviral Response. *Virus Res* **2018**, *256*, 107–116, doi:10.1016/j.virusres.2018.08.008.
19. Kalra, A.; Yetiskul, E.; Wehrle, C.J.; Tuma, F. Physiology, Liver. [Updated 2023 May 1]. In *In: StatPearls [Internet]. Treasure Island (FL): StatPearls Publishing. Available from: https://www.ncbi.nlm.nih.gov/books/NBK535438/* ; 2023.
20. Mahmoud, A.; Al-Rasheed, N.; Hasan, I.; Al-Amin, M.; Al-Ajmi, H.; Al-Rasheed, N. Sitagliptin Attenuates Cardiomyopathy by Modulating the JAK/STAT Signaling Pathway in Experimental Diabetic Rats. *Drug Des Devel Ther* **2016**, *Volume 10*, 2095–2107, doi:10.2147/DDDT.S109287.
21. McInnes, I.B.; Liew, F.Y. Cytokine Networks—towards New Therapies for Rheumatoid Arthritis. *Nat Clin Pract Rheumatol* **2005**, *1*, 31–39, doi:10.1038/ncprheum0020.
22. Ambili, R.; Janam, P. A Critique on Nuclear Factor-Kappa B and Signal Transducer and Activator of Transcription 3: The Key Transcription Factors in Periodontal Pathogenesis. *J Indian Soc Periodontol* **2017**, *21*, 350, doi:10.4103/jisp.jisp_301_16.
23. Leonard, W.J. Role of Jak Kinases and STATs in Cytokine Signal Transduction. *Int J Hematol* **2001**, *73*, 271–277, doi:10.1007/BF02981951.
24. Kudur, M.; Hulmani, M. Rebamipide: A Novel Agent in the Treatment of Recurrent Aphthous Ulcer and Behcet's Syndrome. *Indian J Dermatol* **2013**, *58*, 352, doi:10.4103/0019-5154.117298.
25. Matysiak-Budnik, T.; Heyman, M.; Mégraud, F. Review Article: Rebamipide and the Digestive Epithelial Barrier. *Aliment Pharmacol Ther* **2003**, *18*, 55–62, doi:10.1046/j.1365-2036.18.s1.6.x.
26. Haruma, K.; Ito, M. Review Article: Clinical Significance of Mucosal-protective Agents: Acid, Inflammation, Carcinogenesis and Rebamipide. *Aliment Pharmacol Ther* **2003**, *18*, 153–159, doi:10.1046/j.1365-2036.18.s1.17.x.
27. Tanigawa, T.; Watanabe, T.; Ohkawa, F.; Nadatani, Y.; Otani, K.; Machida, H.; Okazaki, H.; Yamagami, H.; Watanabe, K.; Tominaga, K.; et al. Rebamipide, a Mucoprotective Drug, Inhibits NSAIDs-Induced Gastric Mucosal Injury: Possible Involvement of the Downregulation of 15-Hydroxyprostaglandin Dehydrogenase. *J Clin Biochem Nutr* **2011**, *48*, 149–153, doi:10.3164/jcbn.10-75.
28. Arakawa, T.; Watanabe, T.; Fukuda, T.; Yamasaki, K.; Kobayashi, K. Rebamipide, Novel Prostaglandin-Inducer, Accelerates Healing and Reduces Relapse of Acetic Acid-Induced Rat Gastric Ulcer Comparison with Cimetidine. *Dig Dis Sci* **1995**, *40*, 2469–2472, doi:10.1007/BF02063257.
29. Yoshida, N.; Yoshikawa, T.; Iinuma, S.; Arai, M.; Takenaka, S.; Sakamoto, K.; Miyajima, T.; Nakamura, Y.; Yagi, N.; Naito, Y.; et al. Rebamipide Protects against Activation of Neutrophils ByHelicobacter Pylori. *Dig Dis Sci* **1996**, *41*, 1139–1144, doi:10.1007/BF02088229.
30. Sakurai, K.; Sasabe, H.; koga, T.; Konishi, T. Mechanism of Hydroxyl Radical Scavenging by Rebamipide: Identification of Mono-Hydroxylated

Rebamipide as a Major Reaction Product. *Free Radic Res* **2004**, *38*, 487–494, doi:10.1080/1071576042000209808.
31. Yoshikawa, T.; Naito, Y.; Tanigawa, T.; Kondo, M. Free Radical Scavenging Activity of the Novel Anti-Ulcer Agent Rebamipide Studied by Electron Spin Resonance. *Arzneimittelforschung* **1993**, *43*, 363–366.
32. Hahm, K.B.; Park, I.S.; Kim, Y.S.; Kim, J.H.; Cho, S.W.; Lee, S.I.; Youn, J.K. Role of Rebamipide on Induction of Heat-Shock Proteins and Protection Against Reactive Oxygen Metabolite-Mediated Cell Damage in Cultured Gastric Mucosal Cells. *Free Radic Biol Med* **1997**, *22*, 711–716, doi:10.1016/S0891-5849(96)00406-6.
33. Elmansy, R.A.; Seleem, H.S.; Mahmoud, A.R.; Hassanein, E.H.M.; Ali, F.E.M. Correction to "Rebamipide Potentially Mitigates Methotrexate-induced Nephrotoxicity via Inhibition of Oxidative Stress and Inflammation: A Molecular and Histochemical Study." *Anat Rec* **2023**, *306*, 2208–2209, doi:10.1002/ar.25184.
34. Niwa, Y.; Nakamura, M.; Ohmiya, N.; Maeda, O.; Ando, T.; Itoh, A.; Hirooka, Y.; Goto, H. Efficacy of Rebamipide for Diclofenac-Induced Small-Intestinal Mucosal Injuries in Healthy Subjects: A Prospective, Randomized, Double-Blinded, Placebo-Controlled, Cross-over Study. *J Gastroenterol* **2008**, *43*, 270–276, doi:10.1007/s00535-007-2155-4.
35. Min, H.-K.; Kim, J.-K.; Lee, S.-Y.; Kim, E.-K.; Lee, S.H.; Lee, J.; Kwok, S.-K.; Cho, M.-L.; Park, S.-H. Rebamipide Prevents Peripheral Arthritis and Intestinal Inflammation by Reciprocally Regulating Th17/Treg Cell Imbalance in Mice with Curdlan-Induced Spondyloarthritis. *J Transl Med* **2016**, *14*, 190, doi:10.1186/s12967-016-0942-5.
36. Murakami, I.; Zhang, R.; Kubo, M.; Nagaoka, K.; Eguchi, E.; Ogino, K. Rebamipide Suppresses Mite-Induced Asthmatic Responses in NC/Nga Mice. *American Journal of Physiology-Lung Cellular and Molecular Physiology* **2015**, *309*, L872–L878, doi:10.1152/ajplung.00194.2015.
37. Funahashi, Y.; Yoshida, M.; Yamamoto, T.; Majima, T.; Takai, S.; Gotoh, M. Intravesical Application of Rebamipide Suppresses Bladder Inflammation in a Rat Cystitis Model. *Journal of Urology* **2014**, *191*, 1147–1152, doi:10.1016/j.juro.2013.11.026.
38. Ahmed, H.; Shehata, H.; Mohamed, G.; Abo-Gabal, H.; El-Daly, S. Paracetamol Overdose Induces Acute Liver Injury Accompanied by Oxidative Stress and Inflammation. *Egypt J Chem* **2022**, *0*, 0–0, doi:10.21608/ejchem.2022.140587.6153.
39. Amin, K.A.; Mohamed, B.M.; El-wakil, M.A.M.; Ibrahem, S.O. Impact of Breast Cancer and Combination Chemotherapy on Oxidative Stress, Hepatic and Cardiac Markers. *J Breast Cancer* **2012**, *15*, 306, doi:10.4048/jbc.2012.15.3.306.
40. Abdel-Wahab, B.A.; Ali, F.E.M.; Alkahtani, S.A.; Alshabi, A.M.; Mahnashi, M.H.; Hassanein, E.H.M. Hepatoprotective Effect of Rebamipide against Methotrexate-Induced Hepatic Intoxication: Role of Nrf2/GSK-3β, NF-Kβ-P65/JAK1/STAT3, and PUMA/Bax/Bcl-2 Signaling Pathways. *Immunopharmacol Immunotoxicol* **2020**, *42*, 493–503, doi:10.1080/08923973.2020.1811307.
41. SHAABAN, E.; HAMAD, N.; TORRA, D.; TAHA, M. HISTOPATHOLOGICAL AND BIOCHEMICAL ASSESSMENT OF LIVER FIBROSIS INDUCED BY CARBON TETRACHLORIDE ADMINISTARTION IN RAT. *Assiut Vet Med J* **2023**, *69*, 58–70, doi:10.21608/avmj.2023.181348.1111.
42. Mangoura, S.A.; Ahmed, M.A.; Hamad, N.; Zaka, A.Z.; Khalaf, K.A.; Mahdy, M.A. Vildagliptin Ameliorates Intrapulmonary Vasodilatation and Angiogenesis in Chronic Common Bile Duct Ligation-Induced Hepatopulmonary Syndrome in Rat. *Clin Res Hepatol Gastroenterol* **2024**, *48*, 102408, doi:10.1016/j.clinre.2024.102408.
43. James, L.P.; Mayeux, P.R.; Hinson, J.A. ACETAMINOPHEN-INDUCED HEPATOTOXICITY. *Drug Metabolism and Disposition* **2003**, *31*, 1499–1506, doi:10.1124/dmd.31.12.1499.
44. Song, Z.; McClain, C.J.; Chen, T. S-Adenosylmethionine Protects against Acetaminophen-Induced Hepatotoxicity in Mice. *Pharmacology* **2004**, *71*, 199–208, doi:10.1159/000078086.
45. Kumar, V.; Abbas, A.K.A.; ster, J.C. Perkins Robbins and Cotran Pathologic Basis of Disease, Elsevier/Saunders, Philadelphia, PA. *Elsevier/Saunders, Philadelphia, PA* **2015**, 96–104.
46. Rotundo, L.; Pyrsopoulos, N. Liver Injury Induced by Paracetamol and Challenges Associated with Intentional and Unintentional Use. *World J Hepatol* **2020**, *12*, 125–136, doi:10.4254/wjh.v12.i4.125.
47. Mahmood, N.D.; Mamat, S.S.; Kamisan, F.H.; Yahya, F.; Kamarolzaman, M.F.F.; Nasir, N.; Mohtarrudin, N.; Tohid, S.F.Md.; Zakaria, Z.A. Amelioration of Paracetamol-Induced Hepatotoxicity in Rat by the Administration of Methanol Extract of *Muntingia Calabura* L. Leaves. *Biomed Res Int* **2014**, *2014*, 1–10, doi:10.1155/2014/695678.
48. Arakawa, T.; Kobayashi, K.; Yoshikawa, T.; Tarnawski, A. Rebamipide: Overview of Its Mechanisms of Action and Efficacy in Mucosal Protection and Ulcer Healing. *Dig Dis Sci* **1998**, *43*, 5S-13S.
49. Paul, W.E. Pleiotropy and Redundancy: T Cell-Derived Lymphokines in the Immune Response.

Cell **1989**, *57*, 521–524, doi:10.1016/0092-8674(89)90121-9.
50. Leonard, W.J. The Defective Gene in X-Linked Severe Combined Immunodeficiency Encodes a Shared Interleukin Receptor Subunit: Implications for Cytokine Pleiotropy and Redundancy. *Curr Opin Immunol* **1994**, *6*, 631–635, doi:10.1016/0952-7915(94)90152-X.
51. Hsieh, Y.-C.; Frink, M.; Thobe, B.M.; Hsu, J.-T.; Choudhry, M.A.; Schwacha, M.G.; Bland, K.I.; Chaudry, I.H. 17β-Estradiol Downregulates Kupffer Cell TLR4-Dependent P38 MAPK Pathway and Normalizes Inflammatory Cytokine Production Following Trauma-Hemorrhage. *Mol Immunol* **2007**, *44*, 2165–2172, doi:10.1016/j.molimm.2006.11.019.
52. Khalaf, N.A.; Shakya, A.K.; Al-Othman, A.; El-Agbar, Z.; Farah, H. Antioxidant Activity of Some Common Plants. *Turkish Journal of Biology* **2008**, *32*, 51–55.
53. Higgins, C.P.; Bachne, R.L.; McCallister, J. Polymorpho-Nuclear Leukocyte Species Differences in the Disposal of Hydrogen Peroxide (H2O2). *Proceedings of the Society for Experimental Biology and Medicine* **1978**, *158*, 478–481.
54. Bhushan, B.; Apte, U. Liver Regeneration after Acetaminophen Hepatotoxicity. *Am J Pathol* **2019**, *189*, 719–729, doi:10.1016/j.ajpath.2018.12.006.
55. Fatima, M.; Khan, M.R.; Al-Keridis, L.A.; Alshammari, N.; Patel, M.; Adnan, M.; Sahreen, S. *Pleurospermum Candollei* Methanolic Extract Ameliorates CCl_4 -Induced Liver Injury by Modulating Oxidative Stress, Inflammatory, and Apoptotic Markers in Rats. *ACS Omega* **2023**, *8*, 25999–26011, doi:10.1021/acsomega.3c02031.
56. Zakaria, S.; El-Sisi, A. Rebamipide Retards CCl_4 -Induced Hepatic Fibrosis in Rats: Possible Role for PGE_2. *J Immunotoxicol* **2016**, *13*, 453–462, doi:10.3109/1547691X.2015.1128022.
57. Go, E.K.; Jung, K.J.; Kim, J.M.; Lim, H.; Lim, H.K.; Yu, B.P.; Chung, H.Y. Betaine Modulates Age-Related NF-.KAPPA.B by Thiol-Enhancing Action. *Biol Pharm Bull* **2007**, *30*, 2244–2249, doi:10.1248/bpb.30.2244.
58. Lee, E.K.; Jang, E.J.; Jung, K.J.; Kim, D.H.; Yu, B.P.; Chung, H.Y. Betaine Attenuates Lysophosphatidylcholine-Mediated Adhesion Molecules in Aged Rat Aorta: Modulation of the Nuclear Factor-KB Pathway. *Exp Gerontol* **2013**, *48*, 517–524, doi:10.1016/j.exger.2013.02.024.
59. Ramos-González, E.J.; Bitzer-Quintero, O.K.; Ortiz, G.; Hernández-Cruz, J.J.; Ramírez-Jirano, L.J. Relationship between Inflammation and Oxidative Stress and Its Effect on Multiple Sclerosis. *Neurología* **2024**, *39*, 292–301, doi:10.1016/j.nrl.2021.10.003.
60. Qian, S.; Wei, Z.; Yang, W.; Huang, J.; Yang, Y.; Wang, J. The Role of BCL-2 Family Proteins in Regulating Apoptosis and Cancer Therapy. *Front Oncol* **2022**, *12*, doi:10.3389/fonc.2022.985363.
61. Ahmad, M.M.; Rezk, N.A.; Fawzy, A.; Sabry, M. Protective Effects of Curcumin and Silymarin against Paracetamol Induced Hepatotoxicity in Adult Male Albino Rats. *Gene* **2019**, *712*, 143966, doi:10.1016/j.gene.2019.143966.
62. Kishimoto, S.; Haruma, K.; Tari, A.; Sakurai, K.; Nakano, M.; Nakagawa, Y. Rebamipide, an Antiulcer Drug, Prevents DSS-Induced Colitis Formation in Rats. *Dig Dis Sci* **2000**, *45*, 1608–1616, doi:10.1023/A:1005525313856.
63. Mencin, A.; Kluwe, J.; Schwabe, R.F. Toll-like Receptors as Targets in Chronic Liver Diseases. *Gut* **2009**, *58*, 704–720, doi:10.1136/gut.2008.156307.
64. Du, Z.; Ma, Z.; Lai, S.; Ding, Q.; Hu, Z.; Yang, W.; Qian, Q.; Zhu, L.; Dou, X.; Li, S. Atractylenolide I Ameliorates Acetaminophen-Induced Acute Liver Injury via the TLR4/MAPKs/NF-KB Signaling Pathways. *Front Pharmacol* **2022**, *13*, doi:10.3389/fphar.2022.797499.
65. Chang, C.A.; Akinbobuyi, B.; Quintana, J.M.; Yoshimatsu, G.; Naziruddin, B.; Kane, R.R. Ex-Vivo Generation of Drug-Eluting Islets Improves Transplant Outcomes by Inhibiting TLR4-Mediated NFkB Upregulation. *Biomaterials* **2018**, *159*, 13–24, doi:10.1016/j.biomaterials.2017.12.020.